

Thermoelectric transport in conductive poly(3,4-ethylenedioxythiophene)

Meng Li(李萌), Zuzhi Bai(柏祖志), Xiao Chen(陈晓), Cong-Cong Liu(刘聪聪), Jing-Kun Xu(徐景坤), Xiao-Qi Lan(蓝小琪), and Feng-Xing Jiang(蒋丰兴)

Citation: Chin. Phys. B, 2022, 31 (**2**): 027201. DOI: 10.1088/1674-1056/ac4230

Journal homepage: http://cpb.iphy.ac.cn; http://iopscience.iop.org/cpb

What follows is a list of articles you may be interested in

Thermoelectric transport in conductive poly(3,4-ethylenedioxythiophene)

Meng Li(李萌), Zuzhi Bai(柏祖志), Xiao Chen(陈晓), Cong-Cong Liu(刘聪聪), Jing-Kun Xu(徐景坤), Xiao-Qi Lan(蓝小琪), and Feng-Xing Jiang(蒋丰兴)
Chin. Phys. B, 2022, 31 (**2**): 027201. DOI: 10.1088/1674-1056/ac4230

Thermoelectric enhancement in triple-doped strontium titanate with multi-scale microstructure

Zheng Cao(曹正), Qing-Qiao Fu(傅晴俏), Hui Gu(顾辉), Zhen Tian(田震), Xinba Yaer(新巴雅尔), Juan-Juan Xing(邢娟娟), Lei Miao(苗蕾), Xiao-Huan Wang(王晓欢), Hui-Min Liu(刘慧敏), and Jun Wang(王俊)
Chin. Phys. B, 2021, 30 (**9**): 097204. DOI: 10.1088/1674-1056/abe9a9

Fang-Howard wave function modelling of electron mobility in AlInGaN/AlN/InGaN/GaN double heterostructures

Yao Li(李姚) and Hong-Bin Pu(蒲红斌)
Chin. Phys. B, 2021, 30 (**9**): 097201. DOI: 10.1088/1674-1056/abea87

Twin boundary dominated electric field distribution in CdZnTe detectors

Jiangpeng Dong(董江鹏), Wanqi Jie(介万奇), Jingyi Yu(余竞一), Rongrong Guo(郭榕榕), Christian Teichert, Kevin-P Gradwohl, Bin-Bin Zhang(张滨滨), Xiangxiang Luo(罗翔祥), Shouzhi Xi(席守智), Yadong Xu(徐亚东)
Chin. Phys. B, 2018, 27 (**11**): 117202. DOI: 10.1088/1674-1056/27/11/117202

Coherent charge transport in ferromagnet/semiconductor nanowire/ferromagnet double barrier junctions with the interplay of Rashba spin–orbit coupling, induced superconducting pair potential, and external magnetic field

Li-Jie Huang(黄立捷), Lian Liu(刘恋), Rui-Qiang Wang(王瑞强), Liang-Bin Hu(胡梁宾)
Chin. Phys. B, 2017, 26 (**7**): 077201. DOI: 10.1088/1674-1056/26/7/077201

TOPICAL REVIEW — Organic and hybrid thermoelectrics

Thermoelectric transport in conductive poly(3,4-ethylenedioxythiophene)

Meng Li(李萌)[1,2], Zuzhi Bai(柏祖志)[2], Xiao Chen(陈晓)[1], Cong-Cong Liu(刘聪聪)[2], Jing-Kun Xu(徐景坤)[2], Xiao-Qi Lan(蓝小琪)[1], and Feng-Xing Jiang(蒋丰兴)[1,†]

[1] *Department of Physics, Jiangxi Science & Technology Normal University, Nanchang* 330013, *China*
[2] *Jiangxi Key Laboratory of Flexible Electronics, Jiangxi Science & Technology Normal University, Nanchang* 330013, *China*

(Received 1 October 2021; revised manuscript received 23 November 2021; accepted manuscript online 11 December 2021)

Poly(3,4-ethylenedioxythiophene) (PEDOT) has proved its quite competitive thermoelectric properties in flexible electronics with its excellent electrical and mechanical properties. Since the early discovery of PEDOT, considerable experimental progress has been achieved in optimizing and improving the thermoelectric properties as a promising organic thermoelectric material (OTE). Among them, theoretical research has made significant contributions to its development. Here the basic physics of conductive PEDOT are reviewed based on the combination of theory and experiment. The purpose is to provide a new insight into the development of PEDOT, so as to effectively design and preparation of advanced thermoelectric PEDOT material in the future.

Keywords: PEDOT, charge transport, organic thermoelectric material, structure

PACS: 72.15.Jf, 72.80.Le, 31.15.at, 61.82.Pv **DOI:** 10.1088/1674-1056/ac4230

1. Introduction

Thermoelectric (TE) materials have always been one of the hotspots of scientific research owing to its attractive ability of green energy harvesting, that is, realizing the mutual conversion of heat and electricity without excess emissions. Recently, organic thermoelectric (OTE) material has gained the growing attention due to the strong demand and potential applications in flexible microelectronics, promoting great attention to its thermoelectric performance for environment-friendly energy conversion in spite of the presence of potential challenges.[1–4]

The dimensionless figure of merit (ZT) directly related to the efficiency of thermoelectric energy conversion is usually used to evaluate the thermoelectric performance of materials,

$$ZT = \frac{\sigma S^2}{\kappa} T = \frac{\sigma S^2}{\kappa_{\rm L} + \kappa_{\rm E}} T, \tag{1}$$

where σ, S, κ, and T are the electrical conductivity, Seebeck coefficient (thermopower), thermal conductivity, and absolute temperature, respectively.

The Seebeck coefficient is an open circuit voltage (V) induced by a temperature gradient from hot to cold end of a material, defined as

$$S = -\frac{{\rm d}V}{{\rm d}T}. \tag{2}$$

The negative sign in Eq. (2) represents the type of semiconductor, that is, the gradient direction of the voltage and the temperature gradient are opposite resulting in a positive S, indicating a p-type (hole) semiconductor; reversely, it is an n-type (electron). Seebeck coefficient is a measure of entropy per carrier depending on Femi level ($E_{\rm F}$), where the charge carriers are allowed to participate in transport,[5] and directly relates to the conductivity density of states (DOS), $\sigma(E)$:

$$S = -\frac{k_{\rm B}}{e} \int \frac{E - E_{\rm F}}{k_{\rm B} T} \frac{\sigma(E)}{\sigma} {\rm d}E, \tag{3}$$

where $k_{\rm B}$ is the Boltzmann constant, and e is the charge.

As a promising thermoelectric material, a typical feature of PEDOT is its low thermal conductivity less than ~ 1.0 W·m^{-1}·K^{-1} owing to typically amorphous or semi-crystalline,[6–8] which makes it very close to the characteristics of phonon glass.[5] By considering the difficulty of testing the thermal conductivity of PEDOT films simultaneously, the power factor (σS^2) is usually directly used to evaluate their thermoelectric properties. The thermal conductivity is derived from the contributions of phonons (lattice vibrations, $\kappa_{\rm L}$) and electrons ($\kappa_{\rm E}$)

$$\kappa = \kappa_{\rm L} + \kappa_{\rm E}. \tag{4}$$

For highly doped organic materials, the electronic thermal conductivity can be evaluated by the Wiedemann–Franz law (WFL)

$$\kappa_{\rm E} = L\sigma T, \tag{5}$$

where L is the Lorenz number ($\sim 2.45 \times 10^{-8}$ W·Ω·K^{-2}). Note that, the Lorenz number is allowed to significantly decrease as the bandwidth of the electron or hole dispersion becomes smaller according to theoretical calculation.[9]

Since the discovery of conducting polymers (CPs), particular concern has been paid to them in the field of organic

†Corresponding author. E-mail: f.x.jiang@live.cn

© 2022 Chinese Physical Society and IOP Publishing Ltd

electronics including thermoelectric energy harvesting. In the past half century, on the research of thermoelectric materials, poly(3,4-ethylenedioxythiophene) (PEDOT) has been regarded as one of the most prominent polymers among countless CPs, such as polyaniline, polythiophene, polypyrrole, etc. Recently, many research groups have contributed good reviews to the research and development of thermoelectric PEDOT,[10–13] mainly focusing on material preparation and processing methods as well as the relationship between structure and properties. Remarkable progress on experimental preparation and performance optimization of advanced PEDOT thermoelectrics has been made. Special attention has also been put into its carrier thermoelectric transport theory.[14–16] However, to our best knowledge, there are few reports specifically on PEDOT carrier thermoelectric transport. The purpose of this review is to summarize the current research status and basic physics including thermoelectric transport in PEDOT, aiming to clarify possible ways for the future development of the state-of-the-art OTE materials.

2. Development of thermoelectric PEDOT

PEDOT is one of the first CPs to realize commercial applications, and it plays a crucial role in the field of organic electronics. PEDOT with the oxygen-bearing substituent in thiophene ring allows more stable free radicals and positive charges by further delocalization overcoming the fundamental drawback of polythiophenes which is instability in highly conductive forms in humid air.[17] It is easy to synthesize PEDOT based on its monomer 3,4-ethylenedioxythiophene (EDOT) through simple chemical oxidation or electrochemical oxidation polymerization, as shown in Fig. 1(a). Moreover, its electrical conductivity can span a large range by further oxidation or reduction realizing semiconductor to semi-metallic. The development of synthesis technology (e.g., vapor phase polymerization[18]) continues to contribute to the enhancement of electrical conductivity (> 1000 S·cm^{-1}) owing to improved ordering and stability of PEDOT. Considering solubility and processability, a commercially available poly(3,4-ethylenedioxythiophene): poly(styrenesulfonate) (PEDOT:PSS) dispersion was successfully prepared by combining the non-conductive polystyrenesulfonic acid (PSS) as a counterion in water, which further promotes its application.

PEDOT/PEDOT:PSS is fortunate to be a distinctive representative in OTEs (Fig. 1(b)), thanks to its good environmental stability, biocompatibility, mechanical properties, easy preparation and handling as well as high electrical conductivity.[10,19] Before 2000, there were few experimental reports on PEDOT thermoelectric performance, and the dominant work focused on the factors affecting its charge transport property. In 2008, Xu and his co-workers systematically reported the thermoelectric performance of PEDOT:PSS for the first time, including temperature-dependent electrical conductivity, Seebeck coefficient, and thermal conductivity.[6] They found that ZT of PEDOT:PSS gained an enhanced value ($\sim 10^{-3}$) with a low thermal conductivity (0.17 W·m^{-1}·K^{-1}) at room temperature after secondary doping with dimethyl sulfoxide (DMSO) or ethylene glycol (EG). In 2010, they further achieved a high ZT value of 10^{-2} at room temperature by fabricating PEDOT:PSS films.[20] The enhanced thermoelectric performance is attributed to the increased electrical conductivity and the changeless Seebeck coefficient. This is very attractive for improving the thermoelectric properties of materials,

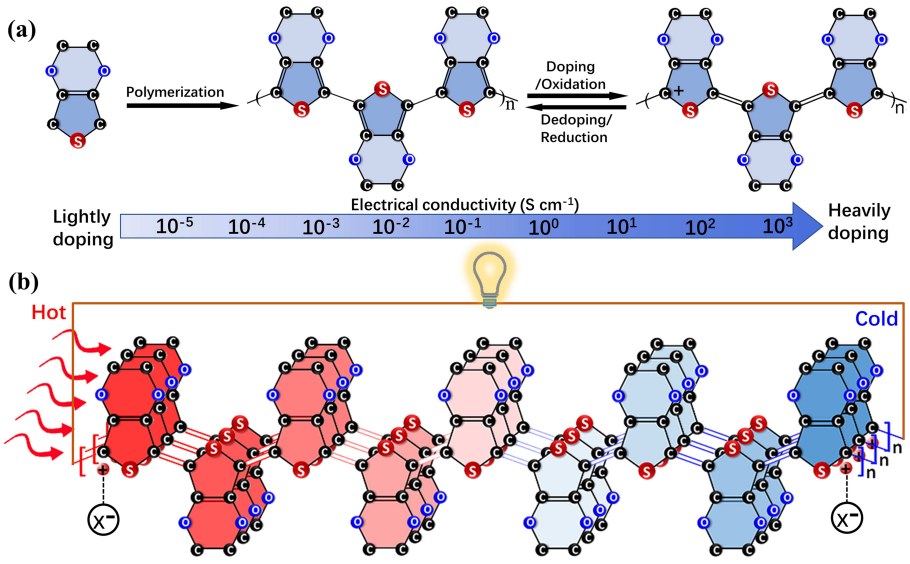


Fig. 1. (a) Schematic of PEDOT obtained by polymerization of EDOT monomers and its neutral (PEDOT) and polaron/bipolaron (PEDOT$^{+/2+}$) states as well as doping-dependent electrical conductivity. (b) Scheme of conductive PEDOT with charge carrier movement under temperature gradient for thermoelectric power generator.

because electrical the conductivity and Seebeck coefficient are generally opposite to the carrier concentration (n). In 2011, Crispin and his co-workers gained a $ZT = 0.25$ at room temperature due to a low in-plane thermal conductivity (0.37 $\mathrm{W{\cdot}m^{-1}{\cdot}K^{-1}}$) by accurate control of the oxidation level in PEDOT exposed to a vapour of tetrakis(dimethylamino)ethylene (TDAE) molecules.[7] In 2013, Pipe *et al.*[21] further increased the ZT of PEDOT to 0.42 at room temperature by reducing the dopant volume of PSS with EG treatment to effectively optimize the carrier concentration. In 2021, Bao and her-coworkers achieved an upper bound for the room temperature ZT of 0.81 for PEDOT:PSS with the high power factor (800 $\mu\mathrm{W{\cdot}m^{-1}{\cdot}K^{2}}$) and the low in-plane thermal conductivity (~ 0.31 $\mathrm{W{\cdot}m^{-1}{\cdot}K^{-1}}$) by a combination of solution-shearing deposition and directionally applied solvent treatments. Over the past ten years, the continuous refresh and improvement of ZT for PEDOT have been witnessed. However, it is still the key issue for PEDOT to further improve its power factor while revealing its mechanism.

Advanced theory is the most powerful tool for early exploration of OTE materials to provide significant support for in-depth optimization and design of high-performance PEDOT. Presently, the computational investigation for thermoelectric transport focused on crystals or highly ordered model systems to predict thermoelectric performance of PEDOT. Kim and Brédas developed the first comprehensive three-dimensional model by using density functional theory (DFT) methods combined with an extensive analysis of crystallographic data for the geometric and electronic structures of PEDOT in the pristine and doped states.[14] They demonstrated that the ethylenedioxy substitution enabled the planarization of polythiophene backbone and the reduction in intrachain charge carrier effective masses due to the shorter intrachain O$\cdots$S binding (2.96 Å) between adjacent monomeric units than the sum of the van der Waals radii of sulfur and oxygen atoms (3.25 Å),[15] while the crystal of pristine PEDOT had a monoclinic lamellar structure with inclined π-stacks. However, the bandgap reduction observed in experiment was attributed to a stronger destabilization of the valence band ($t = 99$ meV) than the conduction band ($t = 170$ meV) after donor-type substitution. In addition, they found that tosylic acid (Tos) doping resulted in a two-dimensional-like metal PEDOT:Tos crystal and also eliminated the intrastack inclination of the PEDOT chains. Furthermore, Shuai and his coworkers revealed the transition from semiconductor to metal with the increase in doping level of Tos and the dominated scattering by ionized impurity in PEDOT:Tos.[15] At the core of thermoelectric theory is the question of OTE transport composed of two processes of charge and heat transports. For PEDOT, similar to other OTE materials, its thermoelectric transport is more complicated and involves many coefficients including electrical conductivity, Seebeck coefficient, electronic and lattice thermal conductivity, etc. Moreover, the molecular interaction among PEDOT chains is the weak van der Waals force, which gives it a complex microstructure and variable macroscopic transport behavior. Therefore, more advanced theories need to be further developed in order to predict the thermoelectric transport properties of PEDOT more accurately.

3. Band structure

3.1. Orbital energy levels

PEDOT is a typical low-bandgap ($E_g = 1.5$ eV in the undoped state[22]) conjugated polymer from sp^2 hybridization involving the covalent bonding between C–C and C–H atoms in thiophene rings; however, the remaining $2p_z$ orbital forms π (bonding) and π^* (antibonding) orbitals stemming from the coupling of conjugated monomers into a longer polymer chain leading to energy level splitting, so that the wavefunctions of C atoms along the polymer backbone overlap, resulting in the delocalized state and semiconducting properties. Compared to polythiophene, PEDOT exhibits a reduced bandgap due to the impact of the ethylenedioxy substitution on the energies of the frontier levels of the π system. Theoretical calculations have indicated that the pristine (neutral) PEDOT is aromatic-like.[23] Moreover, the C–C bonds in EDOT rings become shorter, while the C=C bonds become longer with the increase in the backbone chain length.

The influence of the donor-type substitution is the destabilization of the highest occupied molecular orbital (HOMO) and the lowest unoccupied molecular orbital (LUMO) levels by comparison of EDOT and thiophene monomers, as shown in Fig. 2. The orbital energy levels have changed apparently to a certain extent owing to the antibonding interactions between the O and backbone C atoms. As expected from the evolution of the electronic structure in EDOT oligomers, the change in orbital energy levels is similar to that of thiophene oligomers,[24] the structural parameters and bandgap become smaller and show convergence with increasing number of EDOT unit cell.[25,26] Note that, a common empirical scaling factor is required for DFT calculations to successful comparison with experiment values owing to a discontinuity in exchange-correlation potentials upon removal/addition of an electron.[14] The experimental HOMO and LUMO energy levels can be extracted from the oxidation/reduction potentials of PEDOT through ultraviolet photoelectron spectroscopy (UPS) or combination of cyclic voltammetry (CV) and optical transitions measurements. Control of the band gap in π-conjugated polymers such as PEDOT is important because low band gap conjugated polymers are of great interest in the optimization of thermoelectric performance for OTE materials.

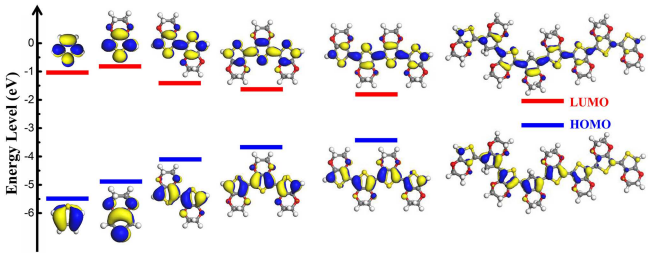


Fig. 2. Evolution of the frontier molecular orbital energies with increasing number of EDOT repeat units. The top and bottom of the plot are the wavefunction patterns in thiophene and EDOT. All the calculations were performed within the generalized gradient approximation (GGA) by using the BLYP exchange–correlation functionals.

3.2. Packing structure

The shape of the electronic structure in pristine PEDOT with isolated chain is similar to that of polythiophene. Its valence band is composed of two dispersive and two flat subbands. Experimental evidence suggests that PEDOT chain backbones can be allowed to adopt a lamellar structure in an orthorhombic unit cell ($a/b/c = 7.935/10.52/7.6$ Å) for both neutral and doped states (Fig. 3).[15,22] In the case of the minimum energy for PEDOT crystal, the rotation angle is 8.9° with a stacking distance of 3.754 Å, leading to a reduction in the total energy by 1.4 kcal/mol per unit cell compared that without rotation between chain backbone and (001) crystal planes.[14] The ethylenedioxy groups in a backbone are still coplanar (*ab* plane) with corresponding thiophene rings by inclining toward the adjacent chains between the lamellar space along the *b* axis in Figs. 3(a) and 3(b). Note that, countless studies have suggested that DFT calculations with experimental lattice constants enable the missing attractive interactions to be effectively compensated, thereby accurately gaining the geometry of molecules, pressure-dependent molecular orientations, intra- and intermolecular vibrational properties within a unit cell.[27,28]

The doped PEDOT:Tos still maintains a good lamellar structure by alternate packing of PEDOT layers and Tos layers along the *a* crystal axis in Figs. 3(c)–3(f).[15] Compared to pristine PEDOT (2.96 Å), the intrachain O···S binding becomes stronger with the smaller distance in lightly (2.91 Å) and heavily (2.89 Å) doped PEDOT:Tos, leading to the significant increase in planarity of PEDOT backbone due to the counterions (Tos). The interchain distance between PEDOT chains in the π–π stacking along the *c* crystal axis gradually decreases in the order of 3.52 Å (pristine) > 3.37 Å (lightly doped) > 3.36 Å (heavily doped), revealing the strong interactions between PEDOT backbones after doping of Tos. Recent experimental data indicate that the monoclinic crystal PEDOT shows the π–π stacking distances of 4.64 Å and 3.4 Å for PEDOT:Cl[29] and PEDOT:PSS,[30] respectively. A larger doping molecule results in a larger chain spacing. Moreover, the moderate doping allows the more ordered packing of PEDOT backbones by forming a quinoid-like structure. Many experimental efforts have confirmed that the quinoid structure (conductive) in doped PEDOT is prone to linear or extended conformation, rather than benzoid structure (neutral) with coiled conformation.[6,31,32] Nevertheless, excessive doping can easily cause the more disordered packing for PEDOT chains leading to degradation of charge transport property, such as PEDOT:PSS (PH1000). This also provides a broad space for optimizing the PEDOT thermoelectric transport properties through adjustment of conformation.

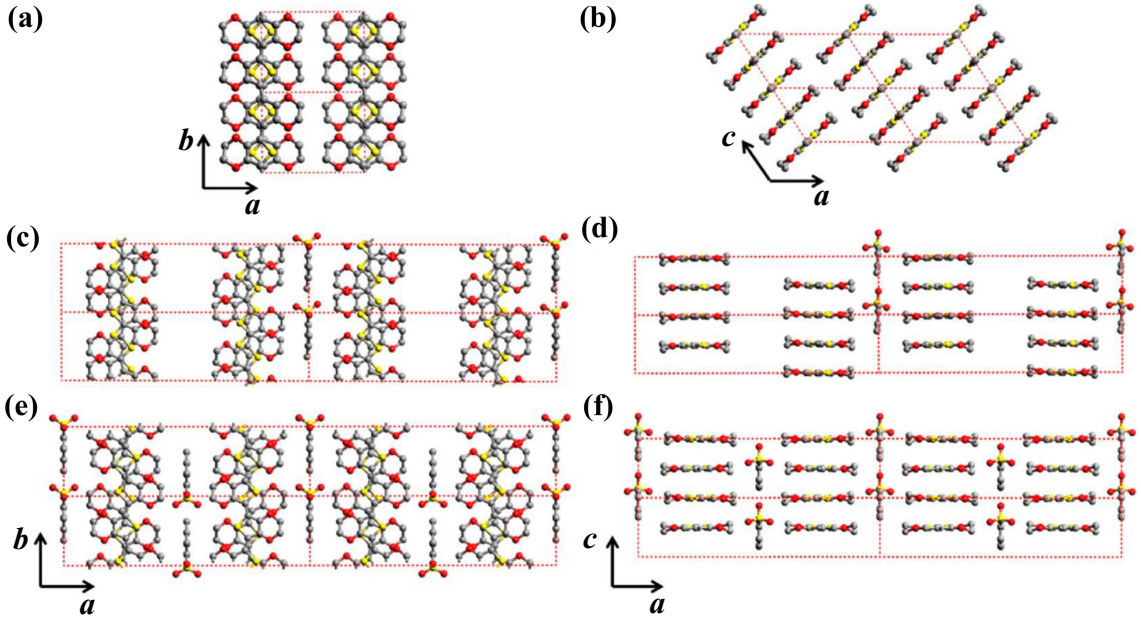


Fig. 3. Calculated structure of the pristine ((a) and (b)), lightly ((c) and (d)), and heavily ((e) and (f)) doped PEDOT crystals. The red dashed lines are the crystal lattices.[15]

3.3. Density of states

The carbon atoms in conjugated polymer backbones are composed of alternating single and double bonds at different length scales. In general, it usually presents linear and coiled as well as its multiphase blend conformations allowing the crystalline, semi-crystalline and amorphous nature due to substrates,[33] preparation method,[30] film thickness,[29] etc. The coiled chains in the conjugated polymer system weaken the overlap of wavefunction between conjugated bonds, resulting in the localized states with various energies. In order to well understand the localized states, the DOS and $E_{\rm F}$ of the polymer system are used to study the electrical conductivity and Seebeck coefficient in homogeneous conjugated polymers. For experimental samples, the PEDOT films are usually composed of 3–10 π–π stacked chain crystallites embedded in the amorphous region of the free-ordered chains.[34] For PEDOT film, its DOS is essentially dictated by the morphology of the film. The derivative $(\mathrm{d}(\ln\sigma(E))/\mathrm{d}E$, Eq. (3)) of DOS at $E_{\rm F}$ is related to the Seebeck coefficient of PEDOT.[16] For heavily doped PEDOT, the $E_{\rm F}$ position locates deeply into the VB substantially leading to the decrease of the Seebeck coefficient. Mũnoz *et al.*[35] proposed a multiscale modeling of electronic structure for PEDOT according to a realistic model of its morphology. They demonstrated that the character of DOS gradually changes from an insulating to a semi-metallic state as the increase of carrier concentration leading to a collapse of the gap between the bipolaron and valence bands. Therefore, the regulation of DOS has become an important means to optimize the thermoelectric performance of PEDOT.

The pristine crystal exhibits that PEDOT is a direct bandgap semiconductor, which can be observed at the Γ-point (Fig. 4(a)).[14] Shuai and his co-workers gave the similar electronic band structure for pristine crystal PEDOT.[15] The interchin interactions in the ΓX zone lead to the increase in bandwidths and reduction in bandgap. The subband splitting in the ΓZ zone indicates that the intrastack interactions along the c axis cause these significant changes. By contrast, the subbands are flat in in the ΓY zone (along the b axis). Also, the electronic coupling in the π-stacking direction is apparently much stronger for the LUMO level than that for the HOMO level owing to the presence of nodes on the sulfur atoms leading to a more limited interchain wavefunction overlap. For the doped PEDOT:Tos crystal (Fig. 4(b)), the $E_{\rm F}$ has shifted into the valence band (VB), indicating a metallic band structure. Moreover, whether it is lightly or heavily doped PEDOT crystals, the similar shift of $E_{\rm F}$ has been evidenced,[15] which is also in agreement with the experimental UPS measurement for both PEDOT:Tos and PEDOT:PSS.[16] However, the crystal with the flat subbands at $E_{\rm F}$ in the ΓY zone is not conducting in the direction perpendicular to the PEDOT layers (the right plots). The metallic nature and orientational anisotropy of the doped PEDOT:Tos conform to the optical reflectance and spectroscopic ellipsometry measurements,[36,37] and are consistent with the significant electrical conductivity.[38] The doping affects both intrachain and interchain bandwidths of PEDOT crystals, more prominently for the latter.[14] These band structures show strong anisotropy due to their lamellar structure, demonstrating the two-dimensional (2D) charge transport in both the pristine and doped PEDOT crystals. Such 2D features are indicative to analyze the coherence of charge transfer in PEDOT crystals thereby assisting in obtaining a new method for optimizing the thermoelectric performance.

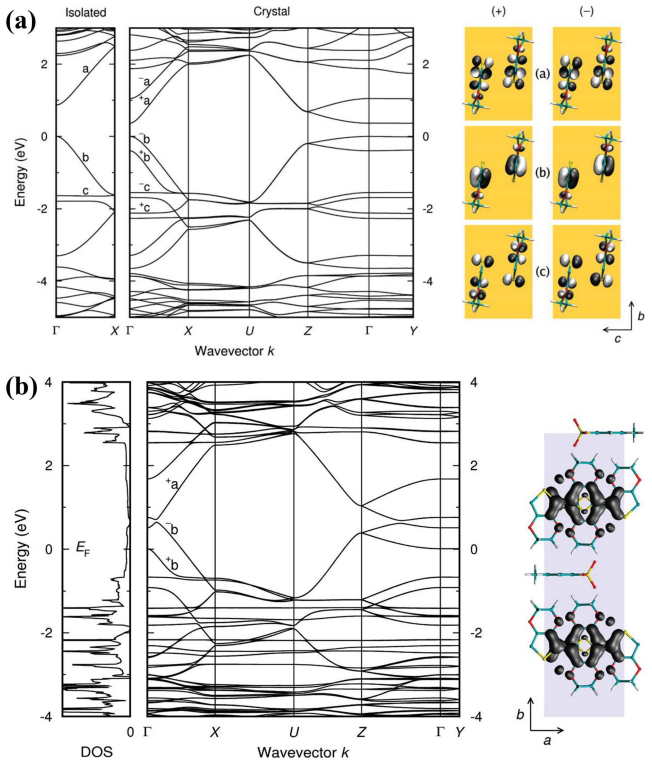


Fig. 4. Band structure and density of states (DOS) of the pristine PEDOT (a) and the PEDOT:Tos (b) crystals. The high symmetry k-points in the first Brillouin zone are $X = (0.5, 0, 0)$, $Y = (0, 0.5, 0)$, $Z = (0, 0, 0.5)$, and $U = (0.5, 0, 0.5)$, respectively. To the right of the plots is an illustration of the charge density at Fermi level ($E_{\rm F}$).[14]

4. Charge transport

4.1. Hopping model

An ideal crystal has translational symmetry. However, when disorder is strong enough, the localization of charges' wavefunctions occurs and the energy band theory is invalid.[39] In the localized state, the metal transforms into an insulator and assumes the Fermi glass state, and the emergence of electrical conductance can only be achieved through thermally activated tunneling or hopping process of charge carriers from a localized site to another. The pioneering work of Mott and Anderson showed that the metal–insulator (MI) phase transition can come from the repulsion between electrons (Mott phase transition) or the localized electron wavefunctions caused by disorder (Anderson phase tran-

sition). Charge transport in PEDOT films is similar to that of other conjugated polymers, such as polyacetylene (PAc), polythiophene (PTh), and polypyrrole (PPy), related to the degree of structural disorder.[40] The PEDOT films usually exhibit the increase in electrical conductivity with the increase of temperature.[6,16] Such behavior indicates that the charge is transported through phonon-induced electron tunneling between localized sites randomly distributed in energy and position through phonons.[41] Note that, the electrical conductivity is independent of the temperature for the impurity scattering, but decreases with the increase of temperature for the case of phonon scattering for the band transport in metals and semiconductors.

The electrical conductivity for conducting polymers including PEDOT films can be evaluated by

$$\sigma = ne\mu. \tag{6}$$

Here, n is the carrier density, e is the electronic charge, and μ is the mobility.

The Mott variable-range hopping between localized states can be described by

$$\sigma_{\mathrm{VRH}}(T) = \sigma_0 \exp[-(T_0/T)^{1/(d+1)}], \tag{7}$$

where σ is a constant with the characteristic of overall conductivity, T_0 related to the activation energy (W) is the energy barrier between localized states, and d is the dimensionality of the transport. In general, the plots of $\ln\sigma$ vs. $1/T$ show a non-liner behavior, but a more nearly straight-line trend for $\ln\sigma$ vs. $T^{-1/4}$ or $T^{-1/2}$ at lightly doped state, indicating the typical transport in disordered and amorphous systems. Heeger *et al.*[42] found that the PEDOT:PSS (Bayer corporation) films exhibited the temperature dependent electrical conductivity ($\sigma_{300\ \mathrm{K}} < 20\ \mathrm{S{\cdot}cm^{-1}}$) with $d \approx 1(1/(d+1)$ is between 0.42 and 0.53) over the temperature range from 300 K to 6 K. Interestingly, this behavior with $d \approx 1$ was also observed for the highly electrical conductivity ($\sim 1000\ \mathrm{S{\cdot}cm^{-1}}$) of PEDOT:PSS films from 300 K to 200 K.[43] A lower T_0 value reveals an easier hopping between PEDOT chains and the less disorder due to the improved intrachain and interchain packing of the PEDOT-rich segments. Note that, various values of d (= 1, 2, and 3) were observed for VRH behavior in PEDOT:PSS, which significantly depends on the processing method, morphology, and microstructure.[44] Nevertheless, the quasi-1D ($d \approx 1$) VRH measured in PEDOT:PSS films continue to account for the majority.

Generally, the hopping model well describes the behavior of charge transport for the early disordered conducting polymers with a relatively low electrical conductivity. However, it is limited in explaining the behavior in highly electrical conductivity in conjugated polymers, such as for the heavily doped or semi-metallic PEDOT. Later, Sheng proposed a new hopping model called fluctuation induced tunneling given in Eq. (8), that is, an electron allows to be removed from a neutral grain and then re-injected to another neighboring one through tunneling,[46]

$$\sigma_{\mathrm{Sheng}}(T) = \sigma_{\mathrm{S}} \exp\left(-\frac{T_1}{T+T_2}\right), \tag{8}$$

here, σ_{S}, T_1, and T_2 are constant, the tunnelling temperatures. T_1 and T_2 depend on the barrier geometry and energy. In this hopping model, energy fluctuations between two close polymer segments are induced via thermal vibrations, resulting in the occurrence of charge tunneling in heavily doped PAc. For the semi-metallic PEDOT,[45] the highly delocalized charges in the first place (Fig. 5(a)) induce the VRH, a less pronounced disorder allows that charges are close enough (Fig. 5(b)) resulting in a local delocalization and the more densely charge zones (polaronic and bipolaronic clusters). The polaronic clusters are allowed to exist in crystalline domains or disordered PEDOT chains. The charge tunneling can occur between two heavily doped segments despite separated by lightly doped ones or excess dopant molecules, e.g., PSS. With the advancement of processing and preparation technologies, it has become increasingly possible to produce well ordered PEDOT films so that coherent transport probably occurs in the absence of the coupling of charge carriers with counter-ions.

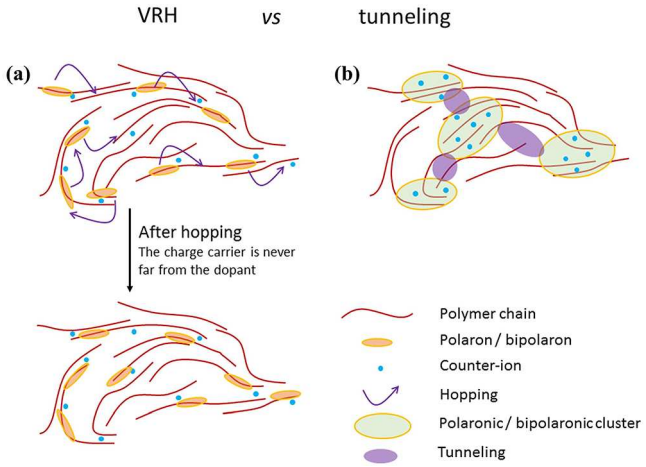


Fig. 5. Schematic diagram illustration of (a) the VRH model vs. (b) the tunneling model.[45]

The hopping transport in PEDOT has been described in detial by Crispin *et al.*[34] Holes belong to polaron ($\mathrm{PEDOT^+}$) or bipolaron ($\mathrm{PEDOT^{2+}}$) bands), and are promoted to the VB with the help of phonon energy, thereby they are allowed to travel through PEDOT film via phonon-assisted hopping between different states. For the VRH, the site where the charge carrier jumps depends on the trade-off between the 'cost' of hopping in real space and hopping in energy space.[40,47] According to the Miller–Abrahams formula, a hopping transport model can be used to describe the electron transport in conducting polymers considering the phonon assisted transition

probability between sites i and j as

$$v_{ij} = \begin{cases} v_0 \exp\left[-\frac{2R}{\alpha} - \frac{E_j - E_i}{kT}\right], & \Delta E = E_j - E_i > 0, \\ v_0 \exp\left[-\frac{2R}{\alpha}\right], & \Delta E \leq 0, \end{cases} \tag{9}$$

where v is the intrinsic attempt-to-hop frequency, ΔE is the energy difference between the sites i (E_i) and j (E_j), R is the distance between sites, and α is the spatial extension of the states participating in the hopping transport (localization length (α) of charge carriers in localized states). A vital and intuitive insight into hopping transport in PEDOT thin films has been achieved from the approach according to the transport energy concept providing simple semi-analytical expressions for electrical conductivity and Seebeck coefficient by using the Monte Carlo technique and the semi-analytical approach, which can be described based on the shapes of the DOS in conducting polymers, the Gaussian distribution by Eq. (10) or Eq. (11),[48–51]

$$g(E) = \frac{N_0}{\sqrt{2\pi}\sigma_{\mathrm{DOS}}} \exp\left(-\frac{E^2}{2\sigma_{\mathrm{DOS}}^2}\right), \tag{10}$$

$$g(E) = \frac{N_0}{2\sigma_{\mathrm{DOS}}} \exp\left(-\frac{|E|}{2\sigma_{\mathrm{DOS}}}\right), \tag{11}$$

where N is the concentration of sites, and σ_{DOS} sets a scale for the energy disorder (the broadening of the DOS). It is worth mentioning that, as to which of these DOS can better reproduce the experimental results, more work is still needed to further confirm. The Seebeck coefficient is given by the expression with the differential conductivity

$$S(T) = \frac{1}{|e|T} \frac{\int \mathrm{d}E(E - E_{\mathrm{F}})\sigma'(E)}{\sigma(T)} = \frac{E_{\mathrm{F}} - E_{\mathrm{tr}}}{|e|T}. \tag{12}$$

Crispin and his co-workers made a comparison between the Monte Carlo and semi-analytical approaches for the conductivity. They found that both approaches exhibit a good qualitative agreement for the concentration dependence of the conductivity and the Seebeck coefficient.[49] The semi-analytical method does not demand extensive computational resources for analyzing the electric and thermoelectric transport in conducting polymers. Its disadvantage is that it relies on many assumptions.[34] However, the validity and accuracy of the semi-analytical approach method allow to be tested against more rigorous calculation techniques, such as the Monte Carlo approach, which is widely used for the calculation of the electron transport in disordered materials. Additionally, Crispin *et al.* present the main steps of the Monte Carlo approach as applied to PEDOT in Ref. [34]. For PEDOT:Tos, the experimental data indicates a hopping model in which localized states correspond to the polaron/bipolaron quasiparticles extended over 2–3 PEDOT monomer units with typical jumps over a distance of 3–4 monomer units. The average hopping distance ($r \approx 3$ nm) extracted from experimental data is similar to the fitting parameters obtained from the Monte Carlo calculation.[7,48]

5. Thermoelectric dependence

5.1. Temperature

Depending on microstructure and doping, PEDOT can be located near the M–I transition. The temperature dependence of the electrical conductivity is an important way to observe the nature of the transport in disordered PEDOT. At a higher temperature than a certain critical one, the Mott dependence can be replaced through the reduced activation energy $W(T)$ in log–log scale by

$$W(T) = \frac{\mathrm{d}\ln\sigma(T)}{\mathrm{d}\ln T} = \frac{\Delta E(T)}{k_{\mathrm{B}}T}, \tag{13}$$

where $E(T)$ is the activation energy characteristic of the transport model. The activation behavior for the electrical conductivity has been observed experimentally[16,54] and theoretically (the Monte Carlo calculations).[49]

The experimental result exhibits the activation energy of 30.3 meV for PEDOT:PSS film, which is in agreement with the calculation result through the Monte Carlo approach (27.5 meV for the Gaussian DOS and 23 meV for the exponential one in Fig. 6(a)). Kim *et al.* compared the $\sigma(T)$ of various PEDOT:PSS (Baytron P) films and demonstrated a quasi one-dimensional (1D) VRH model based on Eq. (7). The slope of $\sigma(T)$, T_0, can be interpreted as an effective energy separation between localized states owing to disorder. The negative slope of temperature dependence of $W(T)$ suggests the insulating regime in PEDOT:PSS films, while the positive slope represents the metallic state. One could notice that the slope for PEDOT:PSS film with DMSO addition in Fig. 6(b) is close to zero implying in the critical regime at the boundary between metallic and insulating states. Noriega *et al.*[53] collected the activation energies (Fig. 6(c)) measured from the temperature-dependent field effect transistors (FET), as well as the trap depth/tail width stemming from modelling electrical transport both from the previous literature and his work. They found that 'classic' semicrystalline and poorly ordered polymers exhibit the significantly lower activation energies and trap breadths than the mean value observed for amorphous conjugated polymers. It has been confirmed that the greater the disorder in conjugated polymers, the deeper the traps and the larger the activation energy. Crispin *et al.*[16] further made a comparison between PEDOT:Tos and PEDOT:PSS and found the opposite relationship of temperature dependences of electrical conductivity in Fig. 6(d). The PEDOT:PSS films show the semiconducting behavior vis a thermally activated transport, while PEDOT:Tos films have the metallic behavior. The distinction in slope of various PEDOT:Tos films indicates a mixed mode of transport simultaneously involving the metallic and the hopping conductions with different weights. The similar behavior has been also observed in ordered PEDOT:PSS film from 200 K to 400 K.[55] The critical temperature appears at 325 K, below which PEDOT:PSS exhibits the semiconducting behavior, while above this value it exhibits metallic properties.

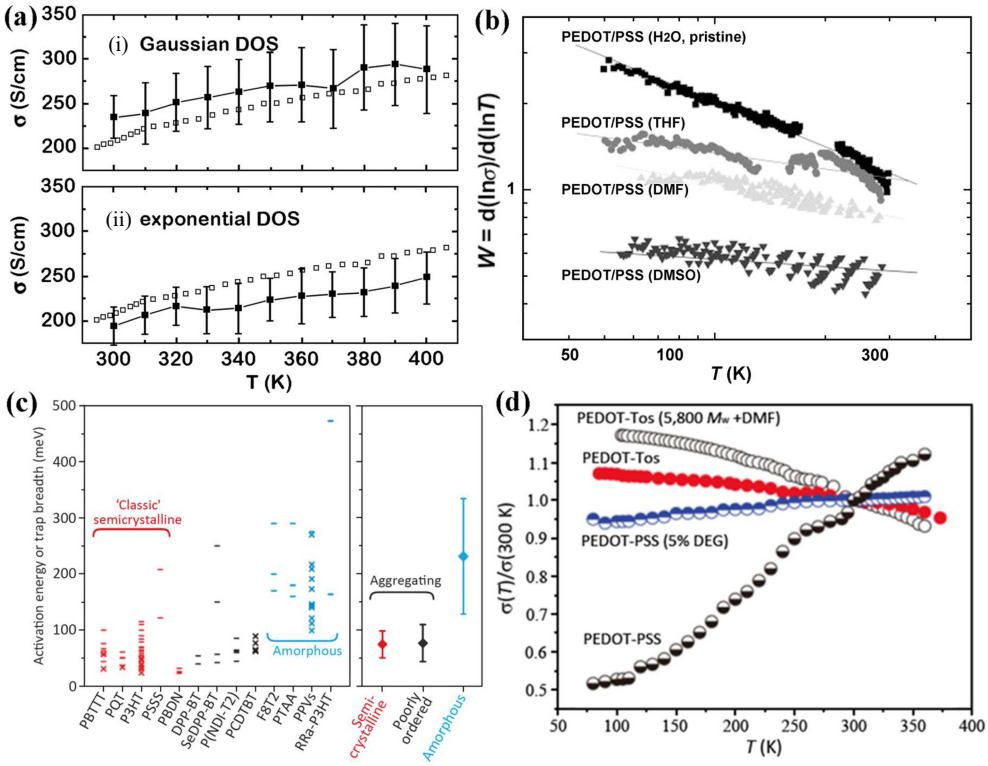


Fig. 6. (a) Monte Carlo calculations of the temperature dependence of the electrical conductivity for the (i) Gaussian and (ii) exponential DOS. The experimental data of Ref. [46] is shown by open squares.[49] (b) Temperature dependences of activation energy (W) of various PEDOT:PSS (Baytron P) films prepared with organic solvents.[52] (c) Activation energy for transport in semiconducting polymers.[53] (d) Temperature dependence of the electrical conductivity (normalized to 300 K) for PEDOT:Tos and PEDOT:PSS films with and without second addition of organic solvents.[16]

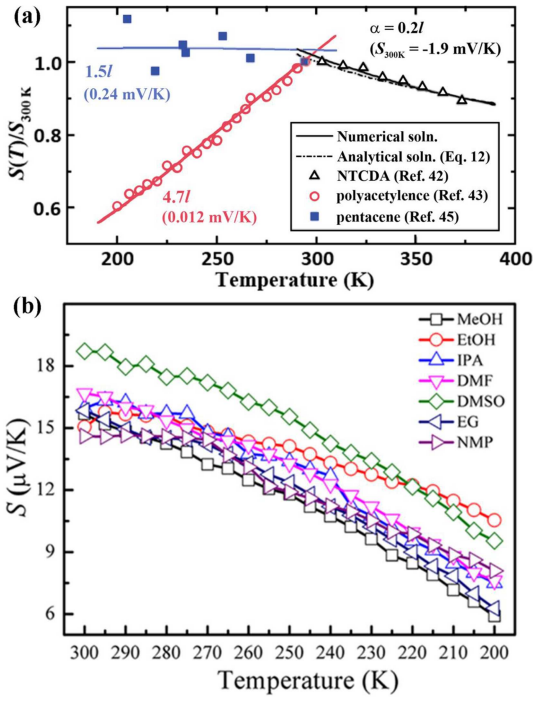


Fig. 7. (a) Fits of the model to further experimental data, demonstrating how $\mathrm{d}|S|/\mathrm{d}T$ changes as α increases from an activated ($|S| \sim 1/T$) regime in NTCDA to an intermediate ($|S| \sim$ const.) regime in pentacene to a VRH ($|S| \sim T$) regime in polyacetylene (PAc).[48] (b) Temperature dependences of Seebeck coefficient of various PEDOT:PSS (PH1000) films prepared via direct dilution-filtration with organic solvents.[43]

The temperature dependence of Seebeck coefficient can be used to characterize the transport likewise in conducting polymers. Pipe and Kim discussed the fit of the model to experimental data by Eq. (12) between Seebeck coefficient and temperature and demonstrated that the relatively delocalized regime is in agreement with VRH transport for PAc.[48] It is evidenced that the model accurately exhibits the approximately linear increase of Seebeck coefficient with temperature in Fig. 7(a). Note that, a temperature-independent behavior of Seebeck coefficient can be also observed due to a lower level of energetic disorder.[56,57] The experimental results have revealed that PEDOT:PSS is a hole transport system and its Seebeck coefficient shows a nearly linear decrease with the decrease of temperature,[6,43] which was also observed in previous report.[52] Moreover, the PEDOT:PSS films with various organic solvents as additives exhibit the enhanced hopping rate compared to pristine film with increase in order. The impact of temperature on Seebeck coefficient is induced by energy disorder, which is similar to PAc with a high energetic disorder.[58]

5.2. Doping/dedoping

In order to optimize the thermoelectric performance of PEDOT, numerous efforts have focused on the precise control of doping levels, including experimental and theoretical calculations. In addition to the influence of energy disorder, the hopping transfer of charge carriers in disordered PEDOT can also be achieved by controlling doping effect in principle. The doping enables PEDOT to achieve the chemical stability in

addition of an electron by a dopant, which can be determined by ionization energy for p-type host polymers (e.g., ~ 5.1 eV for PEDOT:PSS and ~ 5.1 eV for PEDOT:Tos) and the electron affinity for corresponding p-type dopants.[5] Note that, the stability of electron carriers in host polymers depends on their electron affinity which is generally larger than ~ 4 eV to avoid unnecessary chemical reaction with environment (e.g., water and oxygen)[59] and associated trap states.[60] For conducting polymers, polaron effects are related to the doping level. According to Eq. (6), a high electrical conductivity can be gained from the increased doping level for PEDOT crystal. Cho *et al.*[29] estimated the carrier concentration of single-crystal PEDOT nanowires obtained by vapor phase polymerization (VPP) with the doping level of $\sim 10\%$ to be about 6.23×10^{20} cm^{-3} based on the relation

$$n = \frac{dN_{\mathrm{A}}c}{\mathrm{FW}}, \tag{14}$$

where d is the mass density (~ 1.45 g·cm^{-3}), c is the doping level (ionization fraction), N_{A} is Avogadro's number, and FW is mole mass (140 g·mol^{-1}). The as-prepared single-crystal PEDOT nanowires achieved the ultra-high electrical conductivity (8797 S·cm^{-1}) and carrier mobility (88 cm^2·V^{-1}·s^{-1}), which can be attributed to the high crystalline structure involving a small π–π stacking distance.

It has been evidenced by experimental facts that the electrical conductivity of PEDOT films can easily exceed 1000 S·cm^{-1} to achieve semi-metallization by increasing the doping level. The most typical way is through sulfuric acid treatment to realize further doping in PEDOT:PSS ($n > 1 \times 10^{21}$ cm^{-3}).[62–64] Jia *et al.*[65] found that PEDOT:Tos obtained by VPP shows the doping level of 25.2%, and then exhibits the enhanced doping level to 39.7% after sulfuric acid treatment. Note that, the enhanced doping level can also cause changes in the configuration of PEDOT leading to adverse influences on charge transport properties, especially in the presence of inefficient doping, e.g., PEDOT:PSS (discussed below). Ju *et al.*[61] found through DFT calculations that the anions (C(N)) showed the strong influences by the binding energy ΔE of the PEDOT anion complex (Fig. 8(a)), that is, a larger ΔE of PEDOT-C(N) with a longer alkyl tail leading to a stronger polarization of molecule, thereby a greater volumetric occupation of C(N) and a greater reduction in electrostatic interaction between PEDOT and PSS (Fig. 8(b)). With the competitiveness of anions C(N) with PSS counterions, PEDOT-C(N) films overcome the thermoelectric tradeoff relation between Seebeck coefficient and electrical conductivity to achieve their simultaneous enhancement.

It is very useful for the understanding of transport in PEDOT films through studying the thermoelectric parameters dependence of carrier concentration. It is well known that the dependence of Seebeck coefficient and electrical conductivity on the carrier concentration is just the opposite, which greatly hinders the completion of a high thermoelectric power factor (σS^2). In experiments, many efforts can achieve an optimal value of power factor through compromise of them by the control of doping level. Shi *et al.*[15] calculated the thermoelectric transport properties according to the Boltzmann transport equation and the relaxation time approximation by only considering the acoustic phonon scattering of charge carriers in PEDOT (Fig. 9(a)). As expected, contrary to the Seebeck coefficient, the electrical conductivity of PEDOT exhibits the linear increase with the logarithm of the carrier concentration ($n < 1 \times 10^{20}$ cm^{-3}), allowing a maximum of power factor by compromise. The electronic thermal conductivity also shows the linear increase with the carrier concentration. Moreover, the electronic thermal conductivity exhibits a linear relation to the electrical conductivity in Eq. (5).

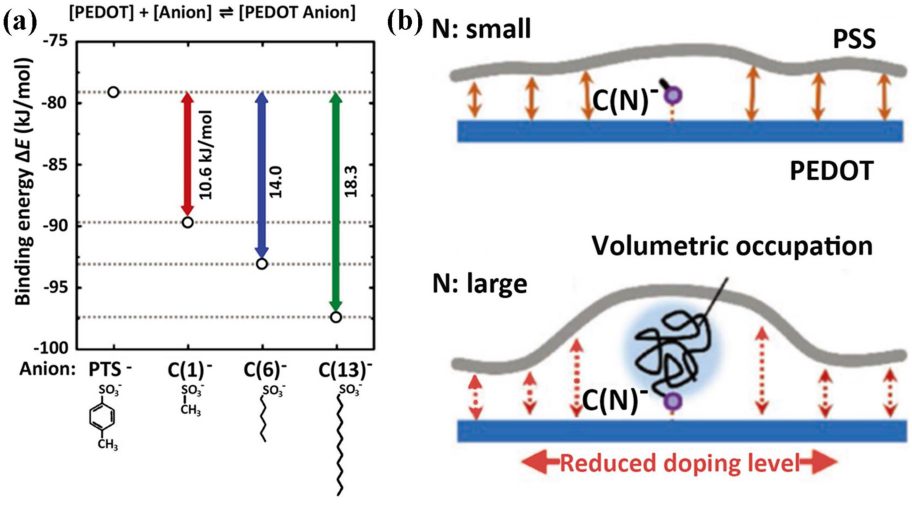


Fig. 8. (a) Binding energy ΔE according to combinations between positively charged PEDOT and different anions C(N) including PTS, C(1), C(6), and C(13). ΔE was calculated by DFT. N is the alkyl chain length. (b) Schemes of electrostatic interaction of PEDOT:PSS added with C(N) when N is small or large.[61]

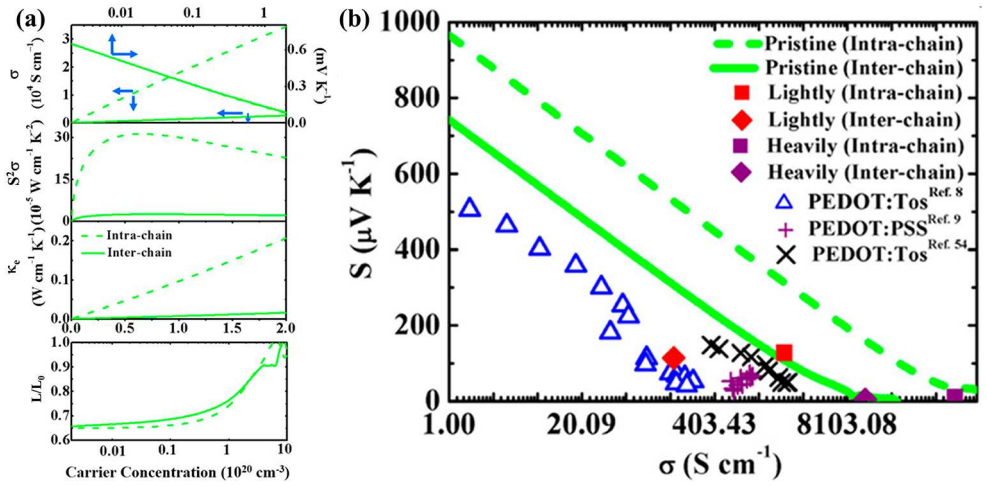


Fig. 9. (a) Electrical conductivity, Seebeck coefficient, power factor, and electronic thermal conductivity of PEDOT as a function of the carrier concentration at 298 K. (b) Seebeck coefficient and logarithm of electrical conductivity relationship for PEDOT with various doping level.[15]

In addition, a linear relationship between the Seebeck coefficient and the logarithm of the electrical conductivity (Fig. 9(b)) has been derived by assuming that the carrier concentration is low and the carriers only transport in on band, defined as[66]

$$S = -\frac{k_B}{e}\ln\sigma_P + \frac{k_B}{e}\ln(N_{eff}e\mu_P). \tag{15}$$

The experimentally measured Seebeck coefficients and the logarithm of the electrical conductivities for PEDOT:Tos show the well-defined linear relationship with a uniform slope $(-k_B/e)$. Compared with the experimental data, the larger intercept for the theoretical prediction indicates an overestimated carrier mobility owing to the neglection of the explicit doping effect.

Recently, the state-of-the-art experiments have mainly focused on the control of doping level for PEDOT to secure a high thermoelectric power factor. For conducting polymers, the carrier concentration depends on the filling (doping) and shape of DOS, while the carrier mobility is related to the shape of DOS.[67,68] In the dominant hopping transport mechanism, the Seebeck coefficient is linked to $E - E_F$ according to Eq. (3). The decrease in the Seebeck coefficient can be attributed to the increase in doping level (c) corresponding to the carrier concentration, resulting in the movement of E_F toward the position of E based on the equation

$$E_F = -\frac{1}{2}\left(\frac{\sigma(E)^2}{k_B T}\right) - k_B T \ln\left(\frac{1}{c}\right). \tag{16}$$

It is evidenced for PEDOT:PSS that the exponential growth of the Seebeck coefficient has been observed with the decreased carrier concentration by using electrochemical gating.[54] This depends on the change in the average energy transported with the charge carriers when filling the DOS. For highly doped PEDOT:PSS, the symmetric in-gap states or bands reveal the presence of polarons/bipolarons. Note that, the width of the (bi)polaronic bands may be predominately due to energy disorder, and some overlap can be observed between the VB and the mixing polaronic/bipolaronic states. In addition, many conducting polymers exhibit the striking empirical relationships between their thermoelectric performance, where $S \propto \sigma^{-1/4}$ and $\sigma S^2 \propto \sigma^{1/2}$.[5,69] However, the two empirical correlations seem not yet applicable to PEDOT. Regardless of the dependent correlation, it has been revealed for PEDOT as the significant strategy to the doping/dedoping optimization in the enhancement of thermoelectric performance.

5.3. Microstructure/morphology

The electronic/hole transport processes are complicated in view of various microstructure for conducting polymers.[5] For highly disordered domain, carrier conduction is generally thermally activated hopping. By contrast, it exhibits the band conduction in highly ordered region. Facts have shown that conducting polymers are neither fully amorphous nor completely crystalline, but the coexistence of semi-ordered and amorphous regions.[70] It has been corroborated in conducting polymers:[71] (i) For the crystalline domains, the thermoelectric power factor is controlled by the electron scattering caused by counterions owing to the strong electrostatic interactions between free charge carriers and counterions; (ii) For the polycrystalline domains, the power factor strongly depends on the crystallite orientations and the grain sizes. Like most conducting polymers, PEDOT generally has a weak inter-chain coupling leading to its intermediate location on the complicated order–disorder microscale.[53] Charge transport in PEDOT is dominated by the disordered regions owing to the limitation of hopping processes.[72] Therefore, the regulation of molecular microstructure in PEDOT/PEDOT:PSS between polycrystalline and amorphous continues to receive considerable attention for enabling high-performance organic thermoelectric materials due to a fundamental grasp of charge transport prop-

erties.

The behaviors of temperature dependent electrical conductivity and Seebeck coefficient (thermopower) are complex with heterogeneous structure, as shown in Fig. 10(a).[5] The charge transport in conducting polymers does not follow a single mechanism, but depends on the weight of ordered and disordered domains in the microstructure (Fig. 10(b)), between (poly)crystalline and amorphous). Kaiser gave the general expressions for the electrical conductivity and Seebeck coefficient by considering a sample composed of two different types of materials in series in the conduction path with σ_1 and σ_2 contributed by the ordered and disordered domains.[73] The total electrical conductivity in heterogeneous media can be defined as

$$\sigma^{-1} = f_1\sigma_1^{-1} + f_2\sigma_2^{-1}, \tag{17}$$

where f_1 and f_2 are the temperature-independent geometrical weighting factors. By contrast, the Seebeck coefficient exhibits more complex behavior.[74]

For a heterogeneous conducting polymer with a high electrical conductivity, the Seebeck coefficient shows significant nonlinear temperature dependence with a knee at low temperatures due to the electron–phonon interaction, which is in agreement with a heterogeneously metallic model.[73] Nevertheless, the behavior of Seebeck coefficient in highly disordered conducting polymers is more in line with VRH model similar to their electrical conductivity. Structure disorder is related to electronic localization due to the molecular stacking and electronic traps, leading to poor electron transport with difficult understanding.[53] Therefore, design and synthesis conjugated polymers with a propensity to crystallize through modification of molecular structure and morphological aggregate referring to the size of macroscopic domains is one of the current significant strategies to improve the electron transport property.

PEDOT has been regarded as a promising candidate due to its linear structure. Thanks to the emergence of oxidative chemical vapor deposition (oCVD), semi-crystal PEDOT films can be easily obtained with relatively high mobility. Sung and his co-workers prepared single-crystal PEDOT nanowires with orthorhombic lattice units resulting in a remarkably high carrier mobility, owing to the decreased lateral chain spacing and π–π stacking distance.[29] Wang *et al.*[76] developed the highly conductive PEDOT thin films with a high mobility by inducing a crystallite-configuration transition using oCVD. High carrier mobility in conducting polymers enables the decrease in energy barrier and the increase in the intercrystallite electron transport.[72] Note that, crystallite size and orientation of ordered domains significantly depend on the deposition temperature and thickness of film as well as substrates.[70,77,78] Franco-Gonzalez and Zozoulenko studied

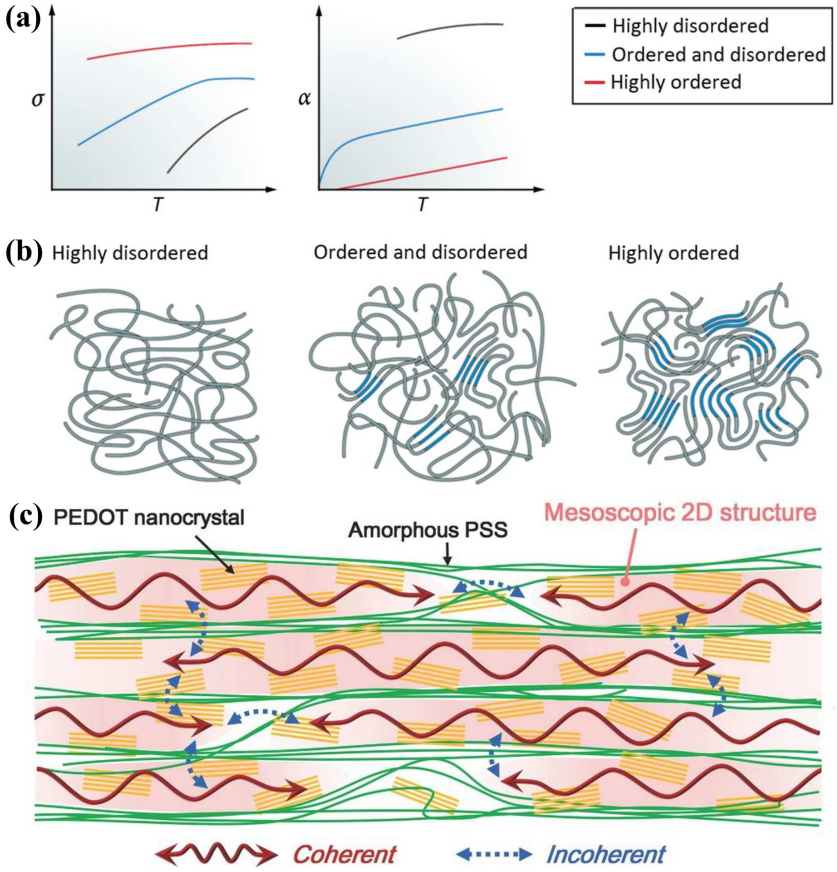


Fig. 10. (a) Temperature dependences of the electrical conductivity (σ) and the thermopower (α) for conducting polymers with (b) highly disordered (left), ordered and disordered (centre), and highly ordered (right) microstructure/morphology.[5] (c) Simplified cross-sectional view of the laminated structure of PEDOT:PSS thin films.[75]

the morphology of PEDOT:Tos and its crystallization in aqueous solution by using atomistic molecular dynamics simulations.[79] It is found that (i) the crystallite PEDOT aggregates are composed of 3–6 π–π stacked chains and linked by interpenetrating to form percolative paths. (ii) The size of PEDOT crystallites is related to water content, but the π–π stacking distance is independent of water content. (iii) Tos counterions are located either on the top of PEDOT chains or the side of crystallites and their distribution depends on the charge concentration. (iv) PEDOT chains and crystallites exhibit bending due to their length and water content. For conventional PEDOT:PSS thick films, Honma *et al.*[75] demonstrated the hieratical nature composed of mesoscopic 2D coherent tunneling and macroscopic 3D hopping among 2D electronic states stemming from nanometer-scale laminated PEDOT nanocrystals, as shown in Fig. 10(c).

In addition, the thermal conductivity of the PEDOT/PEDOT:PSS films exhibits the high anisotropic characteristics due to molecular alignment causing by preparation process and second doping. For the thick (> 20 μm) drop-cast PEDOT films with the in-plane $\sigma > 500$ S·cm^{-1}, the in-plane thermal conductivity ($\kappa_{\parallel}$) is about 1.0 W·m^{-1}·K^{-1}, while the through-plane one ($\kappa_{\perp}$) is about 0.3 W·m^{-1}·K^{-1}.[8] Moreover, different from $\kappa_{\parallel}$ due to a significant electronic contribution, $\kappa_{\perp}$ does not increase with the increase in in-plane σ, which is similar to the thin (~ 100 nm) spin-cast PEDOT:PSS film ($\kappa_{\parallel} \sim 0.29$ W·m^{-1}·K^{-1}). Note that, another explanation for anisotropic thermal conductivity is attributed to the lattice contribution from PSS owing to the orientation of PEDOT chain along the substrate.[80] Therefore, this has also inspired a lot of research on the anisotropic conductance in PEDOT:PSS films by changing conformational/morphological structure of PEDOT and PSS with second additives or post-treatment.[63,64,81–83] For PEDOT/PEDOT:PSS, the theoretical understanding remains insufficient in many aspects for realistic films,[84] such as the DOS, effect of solvents, water, and counterions (dopants), crystallinity and crystallite orientation, length of the conjugation chain on a subnanometer (or even larger) scale. It is expected that more in-depth findings will emerge to elucidate the correlation between the transport properties and structural degrees of freedom in PEDOT/PEDOT:PSS.

6. Conclusion

This review focuses on introducing the current basic physical properties of PEDOT and its progress of thermoelectric performance. Due to the complexity of thermoelectric transport properties, it does not pay attention to all feasible theoretical models and experimental developments. PEDOT has been widely studied as one of the promising organic thermoelectric materials through theory and experiment. The study of PEDOT in thermoelectric performance can not only provide a powerful way to understand the charge transport properties in organic material, but also have laid out a feasible way towards high-performance organic thermoelectric materials. Compared with the commercialized inorganic thermoelectric materials, whether in theory or experiment, PEDOT still addresses the gaps in practical application. It is desired that more efforts would be put into the research of thermoelectric performance on PEDOT to complete a greater progress in the future.

Acknowledgments

Project supported by the National Natural Science Foundation of China (Grant Nos. 51762018, 52073128, and 22065013) and the Natural Science Foundation of Jiangxi Province, China (Grant Nos. 20202ACBL204005, 20202ACBL214005, and 20203AEI003).

References

[1] Zhao W, Ding J, Zou Y, *et al.* 2020 *Chem. Soc. Rev.* **49** 7210
[2] Du Y, Xu J, Paul B, *et al.* 2018 *Appl. Mater. Today* **12** 366
[3] Jia Y, Jiang Q, Sun H, *et al.* 2021 *Adv. Mater.* **33** 2102990
[4] Jiang Q, Sun H, Zhao D, *et al.* 2020 *Adv. Mater.* **32** 2002752
[5] Russ B, Glaudell A, Urban J J, *et al.* 2016 *Nat. Rev. Mater.* **1** 16050
[6] Jiang F, Xu J, Lu B, *et al.* 2008 *Chin. Phys. Lett.* **25** 2202
[7] Bubnova O, Khan Z U, Malti A, *et al.* 2011 *Nat. Mater.* **10** 429
[8] Liu J, Wang X, Li D, *et al.* 2015 *Macromolecules* **48** 585
[9] Jeong C, Datta S and Lundstrom M 2011 *J. Appl. Phys.* **109** 073718
[10] Yue R and Xu J 2012 *Synth. Met.* **162** 912
[11] Fan Z and Ouyang J 2019 *Adv. Electron. Mater.* **5** 1800769
[12] Petsagkourakis I, Kim N, Tybrandt K, *et al.* 2019 *Adv. Electron. Mater.* **5** 1800918
[13] Xu Y, Jia Y, Liu P, *et al.* 2021 *Chem. Eng. J.* **404** 126552
[14] Kim E G and Brédas J L 2008 *J. Am. Chem. Soc.* **130** 16880
[15] Shi W, Zhao T, Xi J, *et al.* 2015 *J. Am. Chem. Soc.* **137** 12929
[16] Bubnova O, Khan Z U, Wang H, *et al.* 2014 *Nat. Mater.* **13** 190
[17] Elschner A, Kirchmeyer S, Lovenich W, Merker U and Reuter K 2011 *PEDOT: Principles and applications of an intrinsically conductive polymer* (CRC Press) p. 41
[18] Winther-Jensen B and West K 2004 *Macromolecules* **37** 4538
[19] Jiang F, Liu C and Xu J 2017 *Chin. Sci. Bull.* **62** 2063
[20] Liu C, Lu B, Yan J, *et al.* 2010 *Synth. Met.* **160** 2481
[21] Kim G H, Shao L, Zhang K, *et al.* 2013 *Nat. Mater.* **12** 719
[22] Aasmundtveit K E, Samuelsen E J, Pettersson L A A, *et al.* 1999 *Synth. Met.* **101** 561
[23] Dkhissi A, Louwet F, Groenendaal L, *et al.* 2002 *Chem. Phys. Lett.* **359** 466
[24] Kroon R, Mengistie D A, Kiefer D, *et al.* 2016 *Chem. Soc. Rev.* **45** 6147
[25] Zade S S and Bendikov M 2006 *Org. Lett.* **8** 5243
[26] Sun H and Autschbach J 2014 *J. Chem. Theory Comput.* **10** 1035
[27] Hummer K, Puschnig P and Ambrosch-Draxl C 2003 *Phys. Rev. B* **67** 184105
[28] Kearley G J, Johnson M R and Tomkinson J 2006 *J. Chem. Phys.* **124** 044514
[29] Cho B, Park K S, Baek J, *et al.* 2014 *Nano Lett.* **14** 3321
[30] Barpuzary D, Kim K and Park M J 2019 *ACS Nano* **13** 3953
[31] Ouyang J, Xu Q, Chu C W, *et al.* 2004 *Polymer* **45** 8443
[32] Atanasov S E, Losego M D, Gong B, *et al.* 2014 *Chem. Mater.* **26** 3471
[33] Franco-Gonzalez J F, Rolland N and Zozoulenko I V 2018 *ACS Appl. Mater. Interfaces* **10** 29115
[34] Kim N, Petsagkourakis I, Chen S, Berggren M, Crispin X, Jonsson M P and Zozoulenko I 2019 *Electric transport properites in PEDOT thin films*, 4th edn. (CRC Press) p. 55

[35] Muñoz W A, Singh S K, Franco-Gonzalez J F, *et al.* 2016 *Phys. Rev. B* **94** 205202
[36] Pettersson L A A, Carlsson F, Inganäs O, *et al.* 1998 *Thin Solid Films* **313-314** 356
[37] Pettersson L A A, Johansson T, Carlsson F, *et al.* 1999 *Synth. Met.* **101** 198
[38] Levermore P A, Chen L, Wang X, *et al.* 2007 *Adv. Mater.* **19** 2379
[39] Heeger A J, Sariciftci N S and Namdas E B 2010 *Semiconducting and metallic polymers* (Oxford University Press) pp. 41–61
[40] Baranovskii S D 2014 *Phys. Status Solidi B* **251** 487
[41] Ambegaokar V, Halperin B I and Langer J S 1971 *Phys. Rev. B* **4** 2612
[42] Aleshin A N, Williams S R and Heeger A J 1998 *Synth. Met.* **94** 173
[43] Xiong J, Jiang F, Zhou W, *et al.* 2015 *RSC Adv.* **5** 60708
[44] Van de Ruit K, Cohen R I, Bollen D, *et al.* 2013 *Adv. Funct. Mater.* **23** 5778
[45] Gueye M N, Carella A, Faure-Vincent J, *et al.* 2020 *Prog. Mater. Sci.* **108** 100616
[46] Sheng P 1980 *Phys. Rev. B* **21** 2180
[47] Vissenberg M C J M and Matters M 1998 *Phys. Rev. B* **57** 12964
[48] Kim G and Pipe K P 2012 *Phys. Rev. B* **86** 085208
[49] Ihnatsenka S, Crispin X and Zozoulenko I V 2015 *Phys. Rev. B* **92** 035201
[50] Maennig B, Pfeiffer M, Nollau A, *et al.* 2001 *Phys. Rev. B* **64** 195208
[51] Schmechel R 2003 *J. Appl. Phys.* **93** 4653
[52] Kim J Y, Jung J H, Lee D E and Joo J 2002 *Synth. Met.* **126** 311
[53] Noriega R, Rivnay J, Vandewal K, *et al.* 2013 *Nat. Mater.* **12** 1038
[54] Bubnova O, Berggren M and Crispin X 2012 *J. Am. Chem. Soc.* **134** 16456
[55] Li Z, Sun H, Hsiao C L, *et al.* 2018 *Adv. Electron. Mater.* **4** 1700496
[56] Venkateshvaran D, Nikolka M, Sadhanala A, *et al.* 2014 *Nature* **515** 384
[57] Von Mühlenen A, Errien N, Schaer M, *et al.* 2007 *Phys. Rev. B* **75** 115338
[58] Park Y W 1991 *Synth. Met.* **45** 173
[59] Anthopoulos T D, Anyfantis G C, Papavassiliou G C, *et al.* 2007 *Appl. Phys. Lett.* **90** 122105
[60] Nicolai H T, Kuik M, Wetzelaer G A H, *et al.* 2012 *Nat. Mater.* **11** 882
[61] Ju D, Kim D, Yook H, *et al.* 2019 *Adv. Funct. Mater.* **29** 1905590
[62] Kim N, Kee S, Lee S H, *et al.* 2014 *Adv. Mater.* **26** 2268
[63] Hosseini E, Kollath O V and Karan K 2020 *J. Mater. Chem. C* **8** 3982
[64] Li X, Liu C, Zhou W, *et al.* 2019 *ACS Appl. Mater. Interfaces* **11** 8138
[65] Jia Y, Liu C, Liu J, *et al.* 2019 *J. Polym. Sci. Poly. Phys.* **57** 257
[66] Shi W, Chen J, Xi J, *et al.* 2014 *Chem. Mater.* **26** 2669
[67] Coropceanu V, Cornil J, Filho D A d S, *et al.* 2007 *Chem. Rev.* **107** 926
[68] Petsagkourakis I, Pavlopoulou E, Cloutet E, *et al.* 2018 *Org. Electron.* **52** 335
[69] Glaudell A M, Cochran J E, Patel S N, *et al.* 2015 *Adv. Energy Mater.* **5** 1401072
[70] Ugur A, Katmis F, Li M, *et al.* 2015 *Adv. Mater.* **27** 4604
[71] Shi W, Yildirim E, Wu G, *et al.* 2020 *Adv. Theory Simul.* **3** 2000015
[72] Jiang F X, Liu C C and Xu J K 2022 *Advanced PEDOT thermoelectric materials* (Elsevier) pp. 257–262
[73] Kaiser A B 1989 *Phys. Rev. B* **40** 2806
[74] Kaiser A B 2001 *Rep. Prog. Phys.* **64** 1
[75] Honma Y, Itoh K, Masunaga H, *et al.* 2018 *Adv. Electron. Mater.* **4** 1700490
[76] Wang X, Zhang X, Sun L, *et al.* 2018 *Sci. Adv.* **4** eaat5780
[77] Dong B X, Wenderott J K and Green P F 2020 *Colloid Polym. Sci.* **299** 439
[78] Rolland N, Franco-Gonzalez J F, Volpi R, *et al.* 2018 *Phys. Rev. Mater.* **2** 045605
[79] Franco-Gonzalez J F and Zozoulenko I V 2017 *J. Phys. Chem. B* **121** 4299
[80] Wei Q, Mukaida M, Kirihara K, *et al.* 2014 *ACS Macro Lett.* **3** 948
[81] Palumbiny C M, Liu F, Russell T P, *et al.* 2015 *Adv. Mater.* **27** 3391
[82] Wei Q, Mukaida M, Naitoh Y, *et al.* 2013 *Adv. Mater.* **25** 2831
[83] Ishibe T, Tomeda A, Komatsubara Y, *et al.* 2021 *Appl. Phys. Lett.* **118** 151601
[84] Zozoulenko I, Franco-Gonzalez J F, Gueskine V, *et al.* 2021 *Macromolecules* **54** 5915